RSC Advances

PAPER

View Article Online
View Journal | View Issue

Cite this: *RSC Adv.*, 2022, **12**, 16599

N,*N*-Dimethylformamide-stabilized ruthenium nanoparticle catalyst for β-alkylated dimer alcohol formation *via* Guerbet reaction of primary alcohols†

Tatsuki Nagata,[a] Kanji Okada,[a] Ryota Kondo,[a] Takashi Toyao,[b] Ken-ichi Shimizu,[b] Takeyuki Suzuki[c] and Yasushi Obora*[a]

Received 13th April 2022
Accepted 26th May 2022

DOI: 10.1039/d2ra02381d

rsc.li/rsc-advances

N,*N*-Dimethylformamide-stabilized Ru nanoparticles (NPs) provide a highly efficient catalyst for the Guerbet reaction of primary alcohols. DMF-modified Ru NPs were synthesized, and characterized by transition electron microscopy, and X-ray absorption spectroscopy, X-ray photoelectronspectroscopy, and Fourier-transform infrared spectroscopy. The Ru NP catalyst was highly durable during catalytic reactions under external additive/solvent-free conditions.

Introduction

Catalytic hydrogen borrowing has attracted considerable interest as a green and atom-economical alkylation process.[1] Owing to the importance of sustainability, minimizing the production of undesired byproducts is important.[2] The Guerbet reaction, which was developed in the 1890s by Marcel Guerbet,[3] produces Guerbet alcohols *via* dehydrative condensation of aliphatic alcohols. Such alcohols are widely used in surfactants, lubricants, and personal care products.[4]

Heterogeneous catalysts,[5] *e.g.*, metals,[6] metal oxides,[7] and metal–organic frameworks,[8] for this transformation have been developed. The harsh reaction conditions required for this reaction and its low selectivity have motivated researchers to develop more-efficient methods for the Guerbet reaction. The use of homogeneous catalysts, *e.g.*, Ir-,[9] Ru-,[10] and Mn[11]-based catalysts, has been investigated. However, the cost and ease of synthesis and handling of highly active ligands and additives have been overlooked.

An alternative approach involves the development of colloidal transition-metal nanoparticle (M NP) catalysts that can be readily prepared *via* a one-step process.[12] Our group has focused on developing a simple method for the synthesis of *N*,*N*-dimethylformamide (DMF)-stabilized M NPs and their use in catalytic reactions. In this method, DMF is used as a reductant, protectant, and solvent. Among various M NPs,[13] Ir NPs show high catalytic activities in the β-benzylation of linear alcohols and β-dimethylation of secondary alcohols with methanol *via* a hydrogen-borrowing process.[14] However, the low abundance and high cost of Ir are drawbacks of this method.

Here, we report the synthesis of DMF-stabilized Ru NPs, their structural characterization, and their use as a catalyst in the Guerbet reaction (homo-β-alkylation) of primary alcohols.

Results and discussion

The DMF-stabilized Ru NPs were synthesized as follows. $RuCl_3 \cdot nH_2O$ was dissolved in hydrochloric acid solution. DMF (50 mL) was added to a 300 mL three-necked round-bottomed flask, and the solution was preheated to 140 °C (±2 °C) and stirred for 5 min. Then a 0.1 M $RuCl_3 \cdot nH_2O$ hydrochloric solution (Ru^{III}) was added to the hot DMF solution. The mixture was stirred (1500 rpm) at 140 °C (±2 °C) for 10 h. The brown solution afforded Ru NPs. The annular dark-field scanning transmission electron microscopy (ADF-STEM) image in Fig. 1 shows the formation of Ru NPs of mean diameter 3.2 nm.

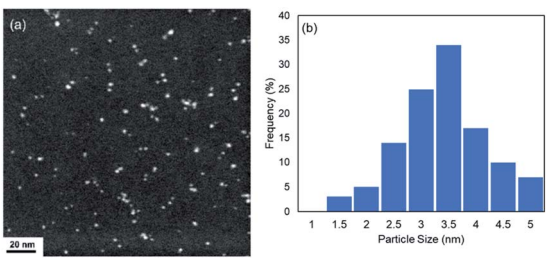

Fig. 1 (a) ADF-STEM image of DMF-stabilized Ru NPs and (b) particle size distribution.

[a]*Department of Chemistry and Materials Engineering, Faculty of Chemistry, Materials, and Bioengineering, Kansai University, Suita, Osaka 564-8680, Japan. E-mail: obora@kansai-u.ac.jp; Fax: +81-6-6339-4026; Tel: +81-6-6368-087*

[b]*Institute for Catalysis, Hokkaido University, N-21, W-10, Sapporo 001-0021, Japan*

[c]*Comprehensive Analysis Center, SANKEN, Osaka University, 8-1 Mihogaoka, Ibaraki, Osaka 567-0057, Japan*

† Electronic supplementary information (ESI) available: Experimental procedures and compound characterization data. See https://doi.org/10.1039/d2ra02381d

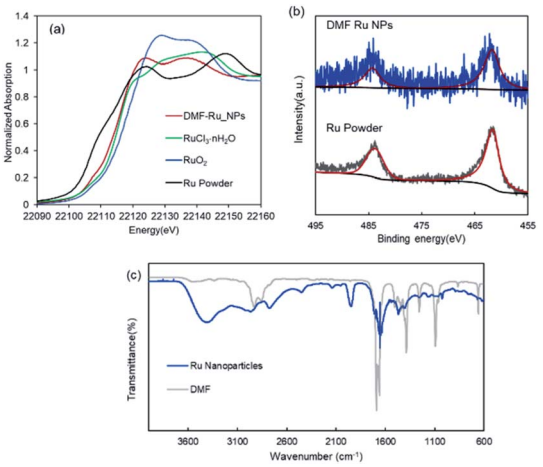

Fig. 2 (a) Ru K-edge XANES spectra of DMF-stabilized Ru NPs (red), RuO_2, and Ru powder; (b) Ru 3p XPS spectra of DMF-stabilized Ru NPs (blue) and Ru powder (gray); and (c) FT-IR spectra of DMF-stabilized Ru NPs (blue) and DMF (gray).

The electronic state of the Ru species in the DMF-stabilized Ru NPs was clarified. The X-ray absorption near-edge structure (XANES) spectrum was compared with those of metallic Ru powder and RuO_2 (Fig. 2a). The absorption edge position of the DMF-stabilized Ru NPs lay between those for metallic Ru and RuO_2, which indicates that reduced Ru species were formed by reduction of the precursor (Ru^{III}). Fig. 2b shows the X-ray photoelectron spectroscopy (XPS) results for the DMF-stabilized Ru NPs. Ru signals ascribed to Ru $3p_{3/2}$, $3p_{1/2}$,and $3d_{5/2}$ are present at 461.5, 444.2, and 280.8 eV, respectively; in the Ru powder spectrum, the signals appear at 461.2 and 279.9 eV, respectively in addition C 1s signals were detected at 284.2, 284.9, 286.0 (Fig. 2b and S1†).[15] Formation of the DMF-stabilized Ru NPs by reduction of the Ru precursor is consistent with the XANES analysis. Fourier-transform infrared (FT-IR) spectra were recorded. Fig. 2c shows the Ru NP spectrum after DMF removal. The absorption peaks for the C=O (1652 cm^{-1}) and C–N (1390 cm^{-1}) vibrational modes of DMF in the spectrum of the DMF-stabilized Ru NPs differ from those in the spectrum of the DMF solvent. The IR absorption attributed to metal carbonyl in the absence of DMF appears at approximately 1950 cm^{-1}. This suggests that CO generated from DMF interacts with metal species.[16]

In this process, DMF acts as a reducing agent at above 100 °C in metal nanoparticle synthesis and the DMF molecules strongly coordinate to the metal center and stabilize the Ru NPs.[13]

Thermogravimetric (TG) analysis was used to investigate the thermal stability of the Ru NPs (Fig. S2†). The TG curves in the range 50–400 °C suggest that the DMF-stabilized Ru NPs were stabilized by various molecules on the surface. The 5% weight loss temperature of the Ru NPs was 190 °C, whereas the decomposition temperature of $Ru_3(CO)_{12}$ was reported in the 160–220 °C range.[17] The decomposition products were identified by thermogravimetry-electron ionization high-resolution time-of-flight mass (TG-EI-HR-TOF MS) analysis of the Ru NPs; H_2O, DMF, CO, CO_2, and dimethylamine were detected (Fig. S3–S5†). These compounds were derived from the Ru NPs. DMF decomposes to give dimethylamine, CO_2 and CO.[18] Four ions (DMF, dimethylamine, CO_2, and CO) were used to analyze the thermal behavior of the Ru NPs. The extracted ion chromatograms of these ions are shown in Fig. S5.† Dimethylamine, which was released around 100–550 °C, is a product of DMF thermal decomposition. DMF was also released at 100–280 °C. Dimethylamine and DMF served as a part of stabilizer. On heating the Ru NPs, a portion of the stabilizers DMF and dimethylamine were expected to be liberated from the Ru metal, generating Ru NPs with partially open sites that could act as active catalysts. Considerable attention must be given to the temperature at which CO is detected because it can also be formed *via* CO_2 fragmentation. CO was detected, not

Table 1 Alkylation of 1-dodecanol with various Ru catalysts[a]

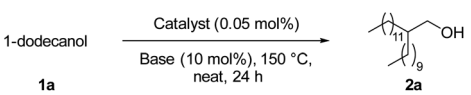

Entry	Ru catalyst	Base	Conv. (%)	Yield[b] (%) (selectivity, %)
1	Ru NPs	KO^tBu	95	93 (98) [83]
2	Ru NPs	KOH	85	83 (98)
3	Ru NPs	Cs_2CO_3	12	2 (17)
4	Ru NPs	K_2CO_3	15	3 (20)
5	$[Ru(p\text{-cymene})Cl_2]_2$	KO^tBu	35	30 (86)
6	$RuCl_2(PPh_3)_3$	KO^tBu	60	55 (92)
7	Ru_3CO_{12}	KO^tBu	47	28 (60)
8	$RuCl_3 \cdot nH_2O$	KO^tBu	40	33 (83)
9	Ru NPs	None	<1	n.d.
10	None	KO^tBu	5	Trace

[a] Reaction conditions: **1a** (2 mmol) was reacted in the presence of a Ru catalyst (0.05 mol%) and base (0.2 mmol) at 150 °C for 24 h. [b] GC yield based on **1a**. Numbers in square brackets show isolated yields. n.d. = not detected by GC. Numbers in parentheses show selectivity of **2a** = [yield (%) **1a**]/[conv. (%) **1a**].

simultaneously with CO_2 and DMF, at approximately 280 °C and above 400 °C. These results suggest partial CO desorption from the Ru NPs.

Next, we investigated the Guerbet reaction of 1-dodecanol (**1a**) as a model substrate under various conditions (Table 1). The reaction of **1a** (2 mmol) was performed in the presence of Ru NPs (0.05 mol%), with KO^{t}Bu (0.2 mmol) as a base, at 150 °C for 24 h; the main β-alkylated product **2a** was obtained in a moderate yield of 93% and with 98% selectivity (Table 1, entry 1). The effect of the base was then determined. A strong base such as KOH gave the desired **2a** in 83% yield, whereas weak inorganic bases such as Cs_2CO_3 and K_2CO_3 were ineffective (Table 1, entries 2–4). Other Ru complexes gave the desired product in moderate yields (Table 1, entries 5–7). Use of the M NP precursor ($RuCl_3 \cdot H_2O$) as the catalyst resulted in a low yield and selectivity (Table 1, entry 8). At this time, the metal black formation significantly decreased catalytic activity. The reaction did not proceed in the absence of a base (Table 1, entry 9) and Ru NPs (Table 1, entry 10). This shows that the catalyst and base are both necessary for alkylation.

The reaction scope was investigated under the optimal reaction conditions (Table 1, entry 1); the results are shown in Fig. 3. The reaction with any C16 to C4 aliphatic primary alcohols gave the corresponding Guerbet alcohols (**2b–2i**). Aliphatic alcohols with short carbon chains resulted in low yields. Similarly, 1-cyclohexylpropanol and tetrahydrogeraniol were efficiently alkylated to give **2j** and **2k** in good yields (74% and 64%, respectively).

The reusability of the Ru NPs was investigated (Fig. 4). The substrates and desired products were removed by distillation (40 Pa, 130 °C). The base was then removed from the mixture by filtering through a cotton plug (for details see Fig. S6†). The Ru NPs retained their catalytic activity and selectivity over several cycles without the need for preactivation.

The feasibility of this transformation was demonstrated by the gram-scale synthesis of **2a** (Fig. 5). Specifically, **1a** (8.8 mmol) was stirred at 150 °C for 48 h in the presence of Ru NPs (0.05 mol%), KO^{t}Bu (0.88 mmol, 10 mol%), which afforded **2a** in good yield (1.22 g). This result supports the scalability of the process.

The Ru NPs were characterized by STEM, X-ray absorption spectroscopy, and XPS to elucidate the reasons for their high catalytic activity. After the 1st reaction, the Ru NP mean diameter had increased slightly to 4.4 nm (Fig. 6a and S7†). The XANES spectrum of the used Ru NPs was similar to that of the fresh Ru NPs (Fig. 6b, green). The Ru $3p_{3/2}$, Ru $3p_{1/2}$, $3d_{5/2}$ peaks of the used Ru NPs appeared at 461.4, 483.7, 280.1 eV, respectively (Fig. S8†). These results suggest that the Ru species in the DMF-stabilized Ru NPs were retained after several uses. The DLS analysis showed that the size of Ru NPs increased after 4th reuse (Fig. S9†). The size increase and aggregation of the metal nanoparticles would decrease the catalytic activity during the recycling process.[19,20]

Fig. 7 shows the time-dependent production of intermediates and the desired products during the Guerbet reaction. The yield of **2a** gradually increased, with low yields of reaction

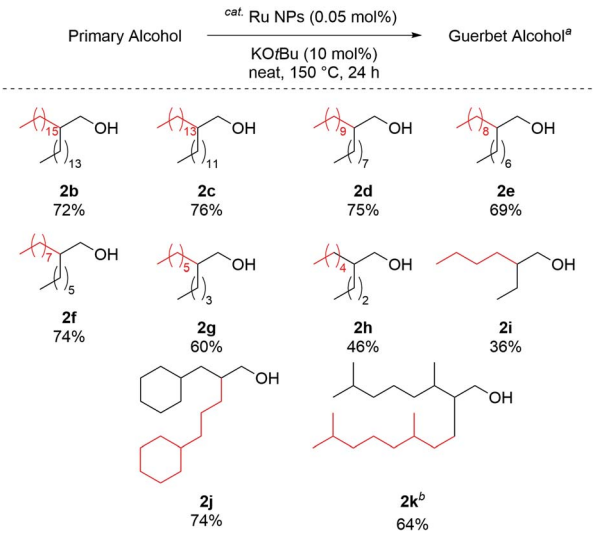

Fig. 3 Substrate scope. [a] Reaction conditions, Table 1, entry 1. [b] 72 h.

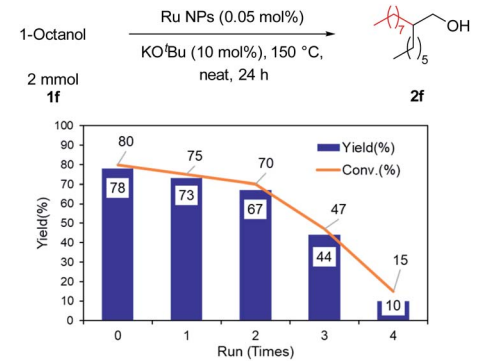

Fig. 4 DMF-stabilized Ru NP reuse in Guerbet reaction of 1-octanol.

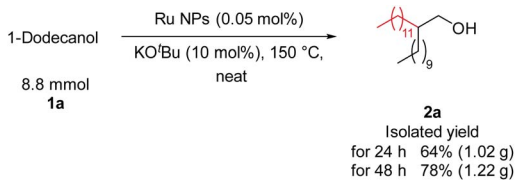

Fig. 5 1 g scale synthesis of **2a**.

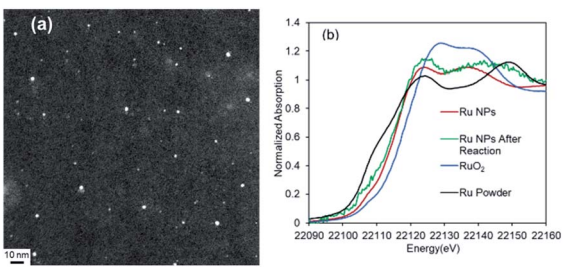

Fig. 6 (a) ADF-STEM image of Ru NPs after reaction and (b) Ru K-edge XANES spectra of Ru NPs before (red) and after reaction (green).

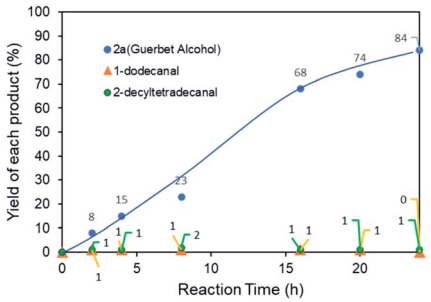

Fig. 7 Time course of reaction with DMF-stabilized Ru NPs.

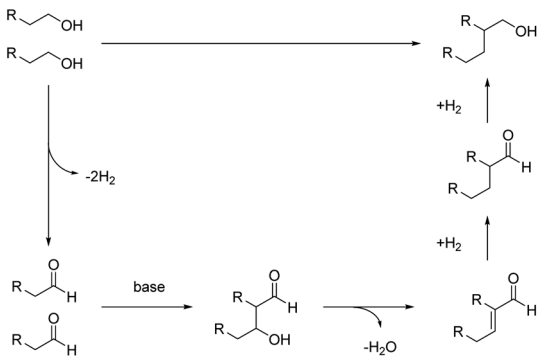

Fig. 8 Plausible reaction pathway for Guerbet reaction with DMF-stabilized Ru NPs.

intermediates such as 1-dodecanal and 1-decyltetradecanal. The produced aldehyde intermediates were immediately consumed. Use of the Ru NP catalyst minimized byproduct formation because of their high dehydrogenation/hydrogenation properties in the Guerbet reaction.[7a,8b]

Based on our experiments, a plausible catalytic mechanism is proposed for the β-alkylation of primary alcohols. As shown in Fig. 8, the primary alcohol is oxidized to give an aldehyde. In the presence of a base, the initially formed aldehydes condense to give the unsaturated aldehyde (aldol condensation). The α,β-unsaturated aldehyde then undergoes hydrogenation in the presence of Ru NPs to generate the desired Guerbet alcohol.

Conclusions

β-Alkylation of primary alcohols to branched alcohols under mild reaction conditions was achieved by using a DMF-stabilized Ru NP catalyst. The Ru NP catalyst promoted the Guerbet reaction under external ligand- and solvent-free conditions. Various primary alcohols were converted into the corresponding branched alcohols in high yields. This catalytic system has significant advantages, namely mild operating conditions, a simple catalyst preparation procedure, high catalyst reusability, and a broad substrate scope. Its use will enable green sustainable Guerbet reactions to be performed.

Conflicts of interest

There are no conflicts to declare.

Acknowledgements

This work was performed by JSPS KAKENHI Grant number 19K05573 and the Research Program for Next Generation Young Scientists of "Five-star Alliance" in "NJRC Mater. & Dev.". High-resolution mass spectra were measured Global Facility Center, Hokkaido University. We thank Y. Murakami and T. Ishibashi of the members of the Comprehensive Analysis Center, and N. Eguchi of the Center of Scientific Instrument Renovation and Manufacturing Support, SANKEN, Osaka University, for TEM, ICP-AES analyses and JEOL Ltd for TG TOF-MS analyses. X-ray absorption measurements were performed at the BL14B2 beamline of SPring-8 at the Japan Synchrotron Radiation Research Institute (JASRI) (No. 2019A1614).

Notes and references

1 (*a*) Y. Obora, *ACS Catal.*, 2014, **4**, 3972; (*b*) B. G. Reed-Berendt, D. E. Latham, M. B. Dambatta and L. C. Morrill, *ACS Cent. Sci.*, 2021, **7**, 570; (*c*) K.-I. Shimizu, *Catal. Sci. Technol.*, 2015, **5**, 1412; (*d*) A. Corma, J. Navas and M. J. Sabater, *Chem. Rev.*, 2018, **118**, 1410.

2 (*a*) H. Li, A. Riisager, S. Saravanamurugan, A. Pandey, R. S. Sangwan, S. Yang and R. Luque, *ACS Catal.*, 2018, **8**, 148; (*b*) A. Kumar, P. Daw and D. Milstein, *Chem. Rev.*, 2022, **122**, 385; (*c*) S. Shylesh, A. A. Gokhale, C. R. Ho and A. T. Bell, *Acc. Chem. Res.*, 2017, **50**, 2589; (*d*) L. Wu, T. Moteki, A. A. Gokhale, D. W. Flaherty and F. D. Toste, *Chem*, 2016, **1**, 32.

3 (*a*) M. Guerbet, *C. R. Hebd. Seances Acad. Sci.*, 1899, **128**, 511; (*b*) A. J. O'Lenick, *J. Surfactants Deterg.*, 2001, **4**, 311.

4 L. D. Rhein, M. Schlossman, A. J. O'Lenick and P. Somasundaran, *Surfactants in Personal Care Products and Decorative Cosmetics*, Taylor & Francis Group, 2007.

5 (*a*) D. Gabriëls, W. Y. Hernández, B. Sels, P. Van Der Voort and A. Verberckmoes, *Catal. Sci. Technol.*, 2015, **5**, 3876; (*b*) J. T. Kozlowski and R. J. Davis, *ACS Catal.*, 2013, **3**, 1588.

6 (*a*) M. Utsunomiya, R. Kondo, T. Oshima, M. Safumi, T. Suzuki and Y. Obora, *Chem. Commun.*, 2021, **57**, 5139; (*b*) X. Zhang, Z. Liu, X. Xu, H. Yue, G. Tian and S. Feng, *ACS Sustainable Chem. Eng.*, 2013, **1**, 1493; (*c*) K. A. Goulas, S. Sreekumar, Y. Song, P. Kharidehal, G. Gunbas, P. J. Dietrich, G. R. Johnson, Y. C. Wang, A. M. Grippo, L. C. Grabow, A. A. Gokhale and F. D. Toste, *J. Am. Chem. Soc.*, 2016, **138**, 6805.

7 (*a*) V. N. Panchenko, E. A. Paukshtis, D. Y. Murzin and I. L. Simakova, *Ind. Eng. Chem. Res.*, 2017, **56**, 13310; (*b*) S. Hanspal, Z. D. Young, H. Shou and R. J. Davis, *ACS Catal.*, 2015, **5**, 1737; (*c*) O. V. Larina, K. V. Valihura, P. I. Kyriienko, N. V. Vlasenko, D. Y. Balakin, I. Khalakhan, T. Čendak, S. O. Soloviev and S. M. Orlyk, *Appl. Catal., A*, 2019, **588**, 117265.

8 (*a*) C. N. Neumann, M. T. Payne, S. J. Rozeveld, Z. Wu, G. Zhang, R. J. Comito, J. T. Miller and M. Dincă, *ACS Appl. Mater. Interfaces*, 2021, **13**, 52113; (*b*) C. N. Neumann, S. J. Rozeveld and M. Dincă, *ACS Catal.*, 2021, **11**, 8521.

9 (*a*) T. Matsu-ura, S. Sakaguchi, Y. Obora and Y. Ishii, *J. Org. Chem.*, 2006, **71**, 8306; (*b*) K. Koda, T. Matsu-ura, Y. Obora and Y. Ishii, *Chem. Lett.*, 2009, **38**, 838; (*c*) G. Xu, T. Lammens, Q. Liu, X. Wang, L. Dong, A. Caiazzo, N. Ashraf, J. Guan and X. Mu, *Green Chem.*, 2014, **16**, 3971; (*d*) S. Chakraborty, P. E. Piszel, C. E. Hayes, R. T. Baker and W. D. Jones, *J. Am. Chem. Soc.*, 2015, **137**, 14264.

10 (*a*) G. R. M. Dowson, M. F. Haddow, J. Lee, R. L. Wingad and D. F. Wass, *Angew. Chem., Int. Ed.*, 2013, **52**, 9005; (*b*) T. A. DiBenedetto and W. D. Jones, *Organometallics*, 2021, **40**, 1884; (*c*) R. L. Wingad, P. J. Gates, S. T. G. Street and D. F. Wass, *ACS Catal.*, 2015, **5**, 5822.

11 (*a*) N. V. Kulkarni, W. W. Brennessel and W. D. Jones, *ACS Catal.*, 2018, **8**, 997; (*b*) A. M. King, H. A. Sparkes, R. L. Wingad and D. F. Wass, *Organometallics*, 2020, **39**, 3873; (*c*) Y. Liu, Z. Shao, Y. Wang, L. Xu, Z. Yu and Q. Liu, *ChemSusChem*, 2019, **12**, 3069.

12 (*a*) Z. B. Shifrina, V. G. Matveeva and L. M. Bronstein, *Chem. Rev.*, 2020, **120**, 1350; (*b*) L. Lu, S. Zou and B. Fang, *ACS Catal.*, 2021, **11**, 6020; (*c*) H. Kawasaki, *Nanotechnol. Rev.*, 2013, **2**, 5.

13 T. Nagata and Y. Obora, *ACS Omega*, 2020, **5**, 98.

14 (*a*) K. Oikawa, S. Itoh, H. Yano, H. Kawasaki and Y. Obora, *Chem. Commun.*, 2017, **53**, 1080; (*b*) M. Kobayashi, H. Yamaguchi, T. Suzuki and Y. Obora, *Org. Biomol. Chem.*, 2021, **19**, 1950.

15 D. J. Morgan, *Surf. Interface Anal.*, 2015, **47**, 1072–1079.

16 (*a*) X. Wang, Y. Hong, H. Shi and J. Szanyi, *J. Catal.*, 2016, **343**, 185; (*b*) S. Y. Chin, C. T. Williams and M. D. Amiridis, *J. Phys. Chem. B*, 2006, **110**, 871.

17 Y. Zhang, C. Zuo, C. Li, X. Guo and S. Zhang, *Green Chem.*, 2016, **18**, 4704.

18 (*a*) T. S. Rodrigues, M. Zhao, T.-H. Yang, K. D. Gilroy, A. G. M. da Silva, P. H. C. Camargo and Y. Xia, *Chem.–Eur. J.*, 2018, **24**, 16944; (*b*) I. Pastoriza-Santos and L. M. Liz-Marzán, *Langmuir*, 1999, **15**, 948; (*c*) J. Y. Yu, S. Schreiner and L. Vaska, *Inorg. Chim. Acta*, 1990, **170**, 145.

19 T. W. Hansen, A. T. Delariva, S. R. Challa and A. K. Datye, *Acc. Chem. Res.*, 2013, **46**, 1720.

20 K. Tabaru, M. Nakatsuji, S. Itoh, T. Suzuki and Y. Obora, *Org. Biomol. Chem.*, 2021, **19**, 3384.